NASA TECHNICAL
MEMORANDUM

NASA TM X-3300

NASA TM X-3300

ADDITION OF OXYGEN TO AND DISTRIBUTION OF OXIDES IN TANTALUM ALLOY T-111 AT LOW CONCENTRATIONS

Stephan Stecura

Lewis Research Center
Cleveland, Ohio 44135

NATIONAL AERONAUTICS AND SPACE ADMINISTRATION • WASHINGTON, D. C. • OCTOBER 1975

1. Report No. NASA TM X-3300	2. Government Accession No.	3. Recipient's Catalog No.

4. Title and Subtitle

ADDITION OF OXYGEN TO AND DISTRIBUTION OF OXIDES IN TANTALUM ALLOY T-111 AT LOW CONCENTRATIONS

5. Report Date
October 1975

6. Performing Organization Code

7. Author(s)

Stephan Stecura

8. Performing Organization Report No.
E-8358

10. Work Unit No.
505-01

9. Performing Organization Name and Address

Lewis Research Center
National Aeronautics and Space Administration
Cleveland, Ohio 44135

11. Contract or Grant No.

13. Type of Report and Period Covered
Technical Memorandum

12. Sponsoring Agency Name and Address

National Aeronautics and Space Administration
Washington, D. C. 20546

14. Sponsoring Agency Code

15. Supplementary Notes

16. Abstract

Oxygen was added to T-111 (Ta-8W-2Hf, wt %) at 820° and 990° C at an oxygen pressure of about 4×10^{-2} N/m^2 (3×10^{-4} torr). The technique permitted predetermined and reproducible doping of T-111 up to 3.0 at. % oxygen. Based on the temperature dependency of the doping reaction, it is concluded that the initial rates of oxygen pickup are probably controlled by solution of oxygen into the T-111 lattice. Although hafnium oxides are more stable than those of tantalum or tungsten, analyses of extracted residues indicate that the tantalum and tungsten oxides predominate in the as-doped specimens, presumably because of the higher concentrations of tantalum and tungsten in the alloy. However, high-temperature annealing promotes gettering of dissolved oxygen and oxygen from other oxides to form hafnium oxides. Small amounts of tantalum and tungsten oxides were still present after high temperature annealing. Tungsten oxide (WO_3) volatilizes slightly from the surface of T-111 at 990° C but not at 820° C. The vaporization of WO_3 has no apparent effect on the doping reaction.

17. Key Words (Suggested by Author(s)) Tantalum alloys T-111 Oxygen dissolution Oxides	18. Distribution Statement Unclassified - unlimited STAR Category 26 (rev.)

19. Security Classif. (of this report) Unclassified	20. Security Classif. (of this page) Unclassified	21. No. of Pages 22	22. Price* $3.25

* For sale by the National Technical Information Service, Springfield, Virginia 22161

ADDITION OF OXYGEN TO AND DISTRIBUTION OF OXIDES IN TANTALUM ALLOY T-111 AT LOW CONCENTRATIONS

by Stephan Stecura

Lewis Research Center

SUMMARY

The T-111 alloy (Ta-8W-2Hf, wt %) was doped with oxygen at 820° and 990° C at an oxygen pressure of about 4×10^{-2} newton per square meter (3×10^{-4} torr). At low oxygen concentrations, doping was reproducible within 0.06 atomic percent, while at higher concentrations (up to 3 at. %) doping was reproducible within 0.11 atomic percent. Based on the temperature dependency of the doping rates, the rate-controlling reaction is probably the solution of oxygen in T-111. At 820° C tungsten oxide (WO_3) formed on specimen surfaces but did not volatilize, and at 990° C tungsten oxide volatilized from the surfaces. The vaporization of WO_3 had no apparent effect on the doping reaction.

Hardness traverses indicated large oxygen concentration gradients in specimens doped at both 820° and 990° C, the gradients being steeper in the 820° C specimens than in the 990° C specimens. A more uniform oxygen distribution was obtained after vacuum annealing at 1320° C for 2 hours.

Although hafnium oxides are more stable than those of tantalum or tungsten, analyses of extracted residues indicate that the tantalum and tungsten oxides predominate in the as-doped specimens, presumably because of the higher concentrations of tantalum and tungsten in the alloy. However, high-temperature annealing promotes gettering of dissolved oxygen and oxygen from other oxides to form a precipitate consisting primarily of halfnium oxides. Small amounts of tantalum and tungsten oxides also were present after high-temperature annealing.

INTRODUCTION

The fabricability, strength, and corrosion resistance of tantalum alloys make them attractive for space-power system applications (refs. 1 and 2). The T-111 alloy (Ta-8W-2Hf, in wt %) is particularly attractive since the presence of hafnium markedly improves its resistance to corrosion by liquid metal working fluids. The T-111 alloy has been studied for containment of isotopic oxide fuels for thermoelectric power generators (ref. 3), for containment of the lithium working fluid in advanced nuclear space-power systems, and for high-temperature heat pipes (refs. 4 to 6).

The T-111 alloy is readily contaminated by oxygen. This contamination affects both its mechanical and physical properties (refs. 7 and 8) and reduces its resistance to corrosion by lithium (ref. 7). Sessions and Devan (ref. 9), however, found that annealing oxygen-doped T-111 at 1300° and 1600° C markedly improved its resistance to corrosion by lithium at 1000° C.

The present study was undertaken to determine the nature of interactions in the oxygen - T-111 system and the resultant distribution of oxygen in T-111 as functions of previous heat treatment, oxygen doping temperature, and high-temperature annealing of oxygen-doped specimens.

EXPERIMENTAL PROCEDURE

Materials

The starting T-111 and Ta-2Hf sheet materials were procured commercially on special order and had the compositions given in table I. The oxygen gas used in these doping experiments contained the following impurities (in ppm by wt): nitrogen, 5; argon, <1; xenon, <1; nitrous oxide (N_2O), <1; and water, <1.

Apparatus

Doping of T-111 was conducted in the apparatus described by Barrett (ref. 11). The amount of oxygen introduced into the quartz doping chamber was measured by sensing the pressure at two separate points in an inlet orifice tube. This pressure differential was electronically integrated with time to produce a reading (in counts) proportional to the amount of oxygen entering the doping chamber and, hence, to the amount of oxygen picked up by the T-111 specimens.

The estimated accuracy of temperature measurements in the resistance heated quartz tube furnace portion of this apparatus was about $\pm 15^{\circ}$ at 990° C.

Procedure

Coupons measuring 3.8 by 2.5 centimeters were machined from 0.10-centimeterthick T-111 and Ta-2Hf sheet materials. The coupons were ultrasonically cleaned in a detergent solution and then etched either in solution A (55 parts conc. H_2SO_4, 25 parts conc. HNO_3, and 20 parts of 49 wt % HF) or in solution B (10 parts conc. H_2SO_4, 25 parts conc. HNO_3, 15 parts of 49 wt % HF, and 40 parts distilled water). All specimens were subsequently thoroughly rinsed in distilled water and in ethyl alcohol and acetone. After cleaning the specimens were vacuum annealed at 1320° C for 2 hours, at 1320° C for 2 hours followed by 930° C for 24 hours, or at 930° C for 24 hours.

The specimens to be doped were suspended by platinum wires from a quartz specimen holder in the doping furnace. The furnace was then evacuated to about 10^{-5} newton per square meter (10^{-7} torr) and slowly heated to the doping temperature so that the pressure in the furnace did not exceed 7×10^{-4} newton per square meter (5×10^{-6} torr) during heating. After stabilization for 1 hour at the doping temperature, low-pressure oxygen was admitted into the furnace through the instrumented orifice, and the coupons were doped at an oxygen pressure of 4×10^{-2} newton per square meter (3×10^{-4} torr).

After doping, some of the coupons were annealed at 1320° C for 2 hours at 10^{-6} newton per square meter (10^{-8} torr). Selected specimens also were studied by X-ray diffraction, microhardness traverses, second-phase extraction and identification, polarized light optical microscopy, and transmission electron microscopy.

RESULTS AND DISCUSSION

Addition of Oxygen

The data in figure 1 illustrate the uniformity of weight gain as a function of oxygen "counts" for the two temperatures employed in this study. Each point in figure 1 corresponds to the weight gain by a separate set of four specimens. The maximum deviation of any point from the average was less than ±5 percent. At low oxygen concentrations (less than 1 atomic percent), doping was reproducible within 0.06 atomic percent; at higher concentrations, up to 3 atomic percent, doping was reproducible within 0.11 atomic percent.

It was assumed that weight gains by the T-111 coupons were due to oxygen pickup. This assumption was confirmed by comparing the inert-gas fusion analyses and the weight gains during doping (table II). The small differences between oxygen contents obtained by these two methods are within the limits of experimental error. The data in table II also show that nitrogen and carbon contents did not change significantly with increasing oxygen content. Hydrogen content was consistently less than 0.003 atomic percent.

The data in figure 2 illustrate the effect of temperature on the doping reaction, the rate of oxygen pickup at 990° C being more rapid than that at 820° C. These curves further show that specimens that were etched in different solutions or annealed at different temperatures for various times before doping had similar rates of oxygen pickup at similar temperatures. Thus, specimen pretreatment had no detectable effect on the rate of oxygen pickup.

Analyses of the weight gain curves in figure 2 indicate that the oxygen doping reactions at both 820° (up to 200 min) and 990° C are essentially linear with time. The data were fit to the equation

$$w = kt^n \tag{1}$$

where w is weight gain (in mg/cm^2), t is time, and k is a constant. Values for the exponent "n" of 0.89 and 0.87 were obtained at 990° and 820° C, respectively. (Strict linearity would be indicated by $n = 1.00$.)

Assuming the reactions to be linear and controlled by the same mechanism at both temperatures, a temperature dependency equivalent to an activation energy of 2.43×10^4 joules per gram mole (5.8 kcal/g mol) is obtained. Since the activation energies for solution and for oxygen diffusion for T-111 are not available, data for unalloyed tantalum were used for comparison. Values for the activation energy for solution of oxygen in tantalum have been reported to be from 3.37×10^3 to 2.43×10^4 joule per gram mole (0.9 to 5.8 kcal/g mol) (refs. 12 to 14); the activation energy for oxygen diffusion is about 1.13×10^5 joule per gram mole (27 kcal/g mol) (ref. 15). Thus, comparing the data obtained in this study with data reported for tantalum, it is concluded that the addition of oxygen to T-111 is probably controlled at least initially by the solution of oxygen rather than by diffusion of oxygen into T-111.

The observed temperature dependence of the doping reaction also is in qualitative agreement with data reported by Inouye (ref. 16), who observed that oxygen weight gains by tantalum and niobium alloys increase with increasing doping temperature. However, Liu, Inouye, and Carpenter (ref. 3) reported that the oxygen doping rate of T-111 was insensitive to temperature between 825° and 1200° C but was proportional to oxygen pressure and inversely proportional to specimen thickness. Their observations concerning the temperature independence of oxygen pickup rates were not confirmed in the present study.

Stringer and Dooley (ref. 17) observed that oxygen doping rates were affected significantly by the geometries of tantalum alloy specimens. The effect of specimen geometry on the doping reaction also was investigated briefly in the present study. Cylinders of T-111 were doped at both 820° and 990° C for comparison with doping rates of flat coupons. The weight gain as a function of time curves for cylindrical specimens were parallel to but slightly lower than the curves for flat coupons shown in figure 2. Thus, the results of Stringer and Dooley were confirmed here by the difference in weight gains between sheet and cylindrical specimens doped under similar conditions.

During the reaction of T-111 with oxygen at 990° C, a white condensate formed on the walls of the quartz furnace tube. This condensate was subsequently identified by X-ray diffraction as WO_3. The amount of tungsten lost as WO_3 during each run was very small, since many sets of specimens had to be doped in order to recover a sufficient amount of this condensate for analysis. No condensate was observed after doping at 820° C.

A binary tantalum alloy, Ta-2Hf, also was doped at 820° and 990° C and an oxygen pressure of 4×10^{-2} newton per square meter (3×10^{-4} torr) for comparison with T-111. The weight gain as a function of time curves for this alloy are shown in figure 3. It was observed that at 990° C the rate of oxygen pickup by Ta-2Hf is essentially the same as that shown for T-111 in figure 2. However, the rate of oxygen pickup by Ta-2Hf at 820° C is about 25 percent greater than that for T-111. Thus, comparison of the doping reactions of T-111 and Ta-2Hf suggests that tungsten in T-111 decreases the reaction rate at 820° C but has no significant effect at 990° C. The data in figure 3 also show that vacuum annealing of Ta-2Hf at 1320° C for 2 hours before doping had no detectable effect on the rate of oxygen pickup.

The temperature dependence of the oxygen doping reaction also was calculated for Ta-2Hf. This temperature dependence corresponded to an activation energy of 7.11×10^{3} joules per gram mole (1.7 kcal/g mol), much less than for T-111. However, the linearity of the reaction and general magnitude of the calculated activation energy suggest that oxygen dissolution also is rate controlling for at least the initial portion (up to 300 min) of the doping reaction for this alloy.

Distribution of Oxygen

Microhardness. - The temperature at which oxygen was added and subsequent heat treatments at 1320° C significantly affected the distribution of oxygen in T-111. Microhardness traverses (fig. 4) show that the oxygen concentration decreases significantly with increasing depth in T-111 after doping at 820° C. Similar results were obtained for specimens doped at 990° C (fig. 5), although the hardness gradients were flatter in these specimens than in the specimens doped at 820° C. These data indicate that the distribution of oxygen in doped T-111 is diffusion controlled under conditions where the overall doping reaction is linear and probably controlled by lattice dissolution of oxygen.

Surface hardness increases rapidly with total oxygen content up to 1.38 atomic percent at 820° C, but increases only slightly with further increases in oxygen content. This behavior suggests that at average oxygen concentrations of about 1.38 atomic percent the surface becomes saturated with oxygen at 820° C. Under these conditions the time dependence of the overall doping reaction could change from linear to parabolic, resulting in deviations from linearity such as observed at 820° C after 200 minutes (fig. 2).

It was further observed that doped specimens vacuum annealed at 1320° C for 2 hours had a lower and more uniform hardness distribution (fig. 6) than the nonannealed specimens (fig. 4). The uniformity of hardness reflects diffusional homogenization of dissolved oxygen during annealing, while the lower hardness indicates a lower concentration of dissolved oxygen.

X-ray diffraction analyses of specimen surfaces. - Lattice dissolution of oxygen in doped T-111 was established by X-ray diffraction, which showed that the lattice parameters increased with increasing oxygen content. These data also showed that annealing of oxygen-doped specimens at 1320° C for 2 hours reduced the lattice parameters for specimens doped to low oxygen contents to about the value for undoped T-111. The lattice parameters for specimens doped to high oxygen contents were decreased to slightly below the value for undoped T-111 by annealing at 1320° C. The decrease in lattice parameters with increasing oxygen content for these doped and annealed specimens is in agreement with observations by Liu, Inouye, and Carpenter (ref. 3) and Harrison and Hoffman (ref. 8). This decrease is attributed to removal of hafnium from solution through the formation of HfO_2 precipitate during high-temperature annealing, as suggested by Liu, Inouye, and Carpenter (ref. 3). Part of this decrease may be due also to removal of tungsten through the formation of volatile tungsten oxide or precipitation of tungsten oxide in the matrix.

The X-ray diffraction patterns from surfaces of specimens doped at 820° C also showed peaks corresponding to a tungsten oxide ($W_{18}O_{49}$). No tungsten oxide peaks were observed on surfaces of specimens doped at 990° C or annealed at 1320° C for 2 hours, reflecting the vaporization of WO_3 from these specimens.

Metallographic studies. - Light optical microscopy studies of oxygen-doped specimens showed that chemical etching in some cases did not reveal second-phase oxide precipitates or only partially revealed grain boundaries and thus was unreliable. In contrast, cathodic etching revealed the microstructures quite adequately. Furthermore, optical polarized-light microscopy and transmission electron-replica microscopy provided more details than light optical microscopy. Consequently, optical polarized-light and transmission electron-replica microscopy studies were done on cathodically etched specimens.

Observations on doped T-111 specimens under polarized light revealed no second phase in the undoped T-111 (containing 0.06 at % oxygen) in either the as-received or annealed condition. However, a second phase was observed in all specimens doped with oxygen at 820° or 990° C. The photomicrographs in figure 7 illustrate the second phase (white dots) and also show that the amount of second phase increases with increasing oxygen content in specimens doped at 820° C. The density of particles also decreased with increasing distance from the surface, further indicating a diffusion-controlled transport mechanism as deduced from hardness traverses. Similar results were obtained with specimens doped at 990° C.

Transmission electron replica microscopy of cathodically etched specimens also was used to characterize the microstructures of oxygen-doped T-111. A micrograph of a specimen doped at 820° C and containing 0.65 atomic percent oxygen shows both large and small intragranular second-phase particles (fig. 8). Such particles were also observed along the grain boundaries. A very unusual arrangement of small particles was also observed along the grain boundaries of this specimen (fig. 9). A greater number of 1.29 atomic percent oxygen (fig. 10). Particles also were observed in this specimen both at grain boundaries and within the grains.

Residue extraction and identification. - To identify oxides formed internally during doping of T-111, selected specimens were dissolved in a methanol - 15-volume-percent bromine solution. No residue was recovered from the undoped T-111 specimen, which contained 0.06 atomic percent oxygen. However, residues were recovered from all other specimens, as indicated in table III. Results from chemical and optical spectrographic analyses indicated that the concentrations of tantalum and tungsten were higher in residues from as-doped specimens than from specimens annealed after doping. Conversely, the concentration of hafnium in residues from annealed specimens was considerably higher than in residues from nonannealed specimens.

The presence of oxide particles in oxygen-doped specimens before and after annealing was confirmed by X-ray diffraction analyses on extracted residues (tables IV and V). The oxides present in these residues were identified by comparison of X-ray diffraction patterns obtained in this study with those reported in references 18 to 29. These analyses showed that the recovered residues probably contained Ta_2O_5, WO_2, WO_3, HfO_2, possibly Ta_6O, Ta_4O, and Ta_2O suboxides, and some strong X-ray diffraction lines (d-spacing values of 1.772, 1.562, 1.515, and 1.001) that could not be indexed with any known oxides of tantalum, tungsten, or hafnium. These unidentified lines were subsequently attributed to Hf_3O, based on the calculated pattern of Hf_3O assuming a structure analogous to Zr_3O (using the data reported in refs. 30 to 33). Therefore, it is concluded that the residues also contained Hf_3O, in addition to the tantalum, tungsten, and hafnium oxides.

The relative content of hafnium oxides in the extracted residues also can be deduced from the X-ray diffraction data. It is apparent from the data in tables IV and V that the number of hafnium oxide X-ray diffraction lines increases with increasing oxygen content and also increases after annealing at 1320° C for 2 hours. This suggests that the amount of hafnium oxide in Ta-111 increased with increasing oxygen content and with annealing, in agreement with analyses of the extracted residues as reported in table III.

Thus, during doping, hafnium did not getter a major portion of oxygen as might have been expected from consideration of the free energies of formation of tantalum, tungsten, and hafnium oxides (ref. 34). However, annealing of oxygen-doped specimens at 1320° C for 2 hours did result in hafnium gettering oxygen from tantalum and tungsten oxides and from solution to form a substantial quantity of hafnium oxides. The gettering of oxygen to form highly stable hafnium oxides is probably the reason Sessions and DeVan (ref. 9) observed such a marked improvement in the resistance of oxygen-doped and annealed T-111 to corrosion by lithium at 1000° C.

SUMMARY OF RESULTS AND CONCLUSIONS

A study was conducted to determine the nature of interactions in the oxygen-T-111 system. The major results and conclusions from this study are:

1. T-111 can be reproducibly doped to predetermined oxygen levels at 820° and 990° C at an oxygen pressure of about 4×10^{-2} newton per square meter (3×10^{-4} torr). Specimen preannealing has no detectable effect on the doping reaction.

2. Based on the relatively low-temperature dependence of the doping reaction, the initial rates of oxygen pickup by T-111 at 820° and 990° C are probably controlled by the solution of oxygen rather than by the diffusion of oxygen in the T-111 alloy matrix.

3. Oxygen distribution is not uniform, and large oxygen concentration gradients are formed in doped T-111. Oxygen was present in doped specimens both in solution and as precipitated oxides. These oxides were primarily oxides of tantalum, with lesser amounts of tungsten and hafnium oxides, reflecting the respective contents of these elements in T-111.

4. Heat treatment of oxygen-doped specimens at 1320° C for 2 hours tends to homogenize the oxygen distribution and promotes the reaction of hafnium with oxygen in solution and with oxides of tantalum and tungsten to form a precipitate consisting primarily of hafnium oxides.

5. Tungsten oxide volatilizes slightly from the surface of T-111 during doping at 990° C and an oxygen pressure of 4×10^{-2} newton per square meter (3×10^{-4} torr) but not at 820° C. The volatilization of tungsten oxide has no apparent effect on the doping reaction.

Lewis Research Center,
National Aeronautics and Space Administration,
Cleveland, Ohio, June 23, 1975,
505-01.

REFERENCES

1. Ammon, R. L.; and Harrod, D. L.: Strengthening Effects in Ta-W-Hf Alloys. WANL-SP-013, Westinghouse Astronuclear Lab., 1966.
2. Recent Advances in Refractory Alloys for Space Power Systems. NASA SP-245, 1969.
3. Liu, C. T.; Inouye, H.; and Carpenter, R. W.: Mechanical Properties and Structure of Oxygen-Doped Tantalum-Base Alloy. ORNL-4839, Oak Ridge National Lab., 1972.
4. Moorehead, Paul E.; and Stone, Philip L.: Survey of Properties of T-111 (Tantalum-8 Tungsten-2 Hafnium). NASA TN D-5873, 1970.
5. Space Power Systems Advanced Technology Conference. NASA SP-131, 1966.
6. Kroeger, Erich W.; Ward, James J.; and Breitwieser, Roland: An Out-Of-Core Version of a Six-Cell Heat-Pipe Heated Thermionic Converter Array. Presented at 7th Intersociety Energy Conversion Engineering Conference, San Diego, Calif., Sept. 25-29, 1972.
7. Hoffman, E. E.; and Harrison, R. W.: The Compatability of Refractory Metals with Liquid Metals. GESP-15, General Electric Co., 1968.
8. Harrison, R. W.; and Hoffman, E. E.: Contamination of Tantalum and Tantalum Alloys in Low Pressure Oxygen Environments. GESP-18, General Electric Co., 1968.
9. Sessions, C. E.; and DeVan, J. H.: Effects of Oxygen, Heat Treatment, and Test Temperature on the Compatability of Several Advanced Refractory Metals and Alloys with Lithium. ORNL-4430, Oak Ridge National Lab., 1971.
10. Kallman, Silve; Hobart, Everett W.; Oberthin, Hans K.; and Brienza, Walter C., Jr.: Determination of Traces of Nitrogen in Refractory Metals and Alloys by Hydrofluoric Acid-Phosphoric Acid-Potassium Dichromate Decomposition and Indophenol Photometry. Anal. Chem., vol. 40, no. 2, Feb. 1968, pp. 332-335.
11. Barrett, Charles A.: Controlled Oxygen Additions to Refractory Metals. NASA TM X-1799, 1969.
12. Parkman, M.; Pape, R.; McRae, R.; Brayton, D.; and Reed, L.: Solubility and Diffusion of Oxygen in Tantalum. NASA CR-1276, 1969.
13. Gebhardt, Erich; and Seghezzi, Hans-Dieter: Untersuchungen in System Tantal-Sauerstoff. II. Reaktionen und Gleichgewichte zwischen Mischkristall-und-Oxydphasen. Zeit. f. Metallkunde, vol. 50, no. 9, 1959, pp. 521-527.

14. Vaughan, Dale A.; Stewart, Oliver M.; and Schwartz, Charles M.: Determination of Interstitial Solid-Solubility Limit in Tantalum and Identification of the Precipitate Phases. AIME Trans., vol. 221, no. 5, Oct. 1961, pp. 937-946.

15. Ang, C. Y.: Activation Energies and Diffusion Coefficients of Oxygen and Nitrogen in Niobium and Tantalum. Acta Met., vol. 1, 1953, pp. 123-125.

16. Inouye, H.: Contamination of Refractory Metals by Residual Gases in Vacuum Below 10^{-6} Torr. ORNL-3674, Oak Ridge National Lab., 1964.

17. Stringer, L.; and Dooley, R. B.: The High Temperature Oxidation of Tantalum-Base Alloys. Proc. Fourth Internatl. Cong. on Met. Corrn., Natl. Assoc. Corrosion Engrs., 1972, pp. 346-352.

18. Brauer, G.; Müller, Horst; and Kühner, G.: Oxide der Tieftemperaturoxydation von Niob und Tantal. J. Less-Common Metals, vol. 4, 1962, pp. 533-546.

19. Schönberg, Nils: An X-ray Investigation of the Tantalum-Oxygen System. Acta Chem. Scand., vol. 8, 1954, pp. 240-245.

20. Steeb, S.; and Renner, J.: Ermittlung der Struktur des Tantalsuboxydes TaOz (Ta_2O) mittels Elektronenbeugung. J. Less-Common Metals, vol. 9, 1965, pp. 181-189.

21. Zaslavskii, A. I.; Zvynchuk, R. A.; and Tutov, A. G.: Rentgenograficheskoe Isledovanie Polymorfyzma Ta_2O_5. Doklady Akademii Nauk SSSR, vol. 104, no. 3, 1955, pp. 409-411.

22. Lehovec, K.: Lattice Structure of Beta-Ta_2O_5. J. Less-Common Metals, vol. 7, 1964, pp. 397-410.

23. Chang, Luke L. Y.; and Phillips, Bert: Phase Relations in Refractory Metal - Oxygen Systems. J. Am. Cer. Soc., vol. 52, Oct. 1969, pp. 527-533.

24. Magneli, Arne; Anderson, Georg; Blomberg, Birgitta; and Kihlborg, Lars: Identification of Molybdenum and Tungsten Oxides. Anal. Chem., vol. 24, no. 12, Dec. 1952, pp. 1998-2000.

25. Vasil'eva, I. A.; Gerasimov, Ya. I.; and Simanov, Yu. P.: The Equilibrium of Tungsten Oxides with Hydrogen. Zhur. Fiz. Khim., vol. 31, 1957, pp. 682-691.

26. Kehl, W. L.; Hay, R. G.; and Wohl, D.: The Structure of Tetragonal Tungsten Trioxide. J. Applied Phys., vol. 23, no. 2, Feb. 1952, pp. 212-215.

27. Curtis, C. E.; Doney, L. M.; and Johnson, J. R.: Properties of Hafnium Oxide, Hafnium Silicate, Calcium Hafnate, and Hafnium Carbide. J. Am. Ceram. Soc., vol. 37, Oct. 1954, pp. 458-465.

28. Geller, S.; and Corenzwit, E.: Hafnium Oxide, HfO_2 (Monoclinic). Anal. Chem., vol. 25, no. 11, Nov. 1953, p. 1774.

29. Adam, J.; and Rogers, M. D.: The Crystal Structure of ZrO_2 and HfO_2. Acta Cryst., vol. 12, 1959, p. 951.

30. Homberg, Bo; and Dagerhamn, Tore: X-ray Studies on Solid Solutions of Oxygen in Beta-Zirconium. Acta Chem. Scand., vol. 15, 1961, pp. 919-925.

31. Samsonov, G. V.: Intermediate Stages in the Formation of Carbides of Titanium, Zirconium, Vanadium, Niobium, and Tantalum. Ukrain. Khim. Zhur., vol. 23, 1957, pp. 287-296.

32. Dagerhamn, Tore: X-ray Study of Solid Solutions of Oxygen in Hafnium. Acta Chem. Scand., vol. 15, 1961, pp. 214-215.

33. Kornilov, I. I.; Glazova, V. V.; and Ruda, G. N.: Formation of the Compounds Hf_6O and Hf_3O in the Hafnium-Oxygen System. Inorg. Mater., vol. 4, no. 12, Dec. 1968, pp. 1830-1833.

34. Wicks, C. E.; and Block, F. E.: Thermodynamic Properties of 65 Elements - Their Oxides, Halides, Carbides, and Nitrides. Bulletin 605, Bureau of Mines, 1963.

TABLE I. - ANALYSES OF TANTALUM T-111 AND Ta-2Hf ALLOYS

Impurity	Concentration, ppm by wt		Impurity	Concentration, ppm by wt	
	T-111	Ta-2Hf		T-111	Ta-2Hf
Carbon[a]	95	88	Cobalt	5	1
Nitrogen[a]	20	23	Copper	1	1
Oxygen[a]	55	62	Iron	50	35
Hydrogen[a]	2	3	Molybdenum	150	140
Hafnium[a]	[b]2.2	[b]2.1	Nickel	10	20
Tungsten[a]	[b]7.9	5	Niobium	250	160
Aluminum	5	4	Silicon	1	5
Boron	1	1	Vanadium	2	1
Chromium	1	1			

[a] Elements determined by chemical analyses. All other elements determined by optical spectrographic analysis.

[b] Values expressed in wt %.

TABLE II. - CONCENTRATION OF OXYGEN IN TANTALUM T-111 ALLOY SAMPLES AS DETERMINED BY WEIGHT DIFFERENCE AND GAS FUSION METHODS

[Oxygen, nitrogen, and carbon were determined by inert-gas fusion, modified Kjeldahl (ref. 10), and combustion methods, respectively.]

Sample	Oxygen concentration, at. %		Nitrogen content, at. %	Carbon content, at. %
	Weight difference	Inert-gas fusion		
1	----	0.06	0.03	0.14
2	0.27	.32	.01	.18
3	.43	.45	.02	.16
4	.65	.62	.02	----
5	.97	.99	.02	.15
6	1.43	1.47	.02	.14
7	2.00	1.90	.02	----
8	2.88	2.65	.02	.14

TABLE III. - OXIDES EXTRACTED FROM OXYGEN-DOPED

TANTALUM ALLOY SAMPLES

Sample	Oxygen concentration, at. %	Doping temperature, °C	Annealing temperature, °C (a)	Elements present in residues, wt %[b]			Oxides present in residues (c)
				Ta	Hf	W	
1	0.06	---	1320	--	--	--	No residue
2	.18	820	1320	50	44	6	Ta-, Hf-, W-oxides
3	.26	↓	----	76	3	18	↓
4	.34		----	72	5	22	
5	.32		1320	40	50	8	
6	.88		----	65	15	16	
7	.92		1320	29	61	9	
8	2.98		1320	25	67	8	
9	.43	990	----	58	18	12	
10	.97	990	1320	23	70	7	

[a] Annealed for 2 hr at 1.3×10^{-6} N/m^2 (10^{-8} torr) pressure.

[b] Analyzed by optical spectrographic and chemical methods.

[c] Oxides identified by X-ray diffraction analyses.

TABLE IV. - X-RAY DIFFRACTION PATTERNS FOR OXIDES EXTRACTED FROM NONANNEALED AND ANNEALED[a] OXYGEN-DOPED T-111 SAMPLES DOPED WITH OXYGEN AT 820° C

Oxygen concentration, at. %	T-111 condition	d-Spacing, Å	Intensity (b)	Oxide
0.25	Nonannealed	6.61	VW	Ta_2O
		3.83	W	Ta_2O; WO_3
		3.67	W	HfO_2; Ta_2O_5
		3.60	W	HfO_2
		3.45	W	WO_2
		2.826	VS	HfO_2
		2.720	S	Ta_2O
		2.343	M	Ta_2O
		2.283	VW	Ta_4O
		2.120	VW	Ta_2O; Ta_2O_5
		2.109	VW	Ta_2O_5
		2.036	W	WO_3
		1.929	VW	Ta_2O
		1.914	VW	WO_3
		1.856	VW	Ta_2O; HfO_2
		1.838	VW	HfO_2; Ta_2O
		1.799	W	Ta_2O_5; Hf_3O
		1.679	W	Ta_6O; HfO_2
		1.600	W	HfO_2; Ta_4O
		1.549	VW	WO_2
		1.539	VW	Ta_2O; HfO_2
		1.428	VW	Ta_2O_5
		1.400	W	WO_2; Ta_2O
		1.367	W	Ta_6O
		1.346	VW	Ta_6O; Ta_4O
		1.305	VW	Ta_2O; TaO_2
		1.036	VW	Ta_6O; Ta_2O
0.18	Annealed	3.62	VW	HfO_2; Ta_4O; WO_3
		3.47	W	WO_2
		3.13	M	HfO_2; Ta_2O_5
		2.960	VW	Ta_2O
		2.827	S	HfO_2; WO_2
		2.717	W	Ta_2O
		2.572	W	TaO_2
		2.483	VW	HfO_2
		2.366	VW	Ta_2O_5
		1.801	W	HfO_2; Ta_4O; WO_3
		1.772	M	Hf_3O
		1.698	VW	WO_2; WO_3
		1.634	VW	HfO_2; Ta_2O_5
		1.562	W	Hf_3O; WO_3
		1.523	VW	Ta_2O
		1.515	M	Hf_3O
		1.469	W	Ta_2O_5; Ta_6O
		1.264	VW	Ta_2O
		1.256	W	HfO_2
		1.172	VW	Ta_6O; Ta_4O
		1.153	VW	Ta_2O
		1.127	VW	Ta_4O
		1.088	VW	HfO_2; WO_3
		1.050	VW	WO_3; HfO_2
		1.033	VW	Ta_2O
		1.001	W	Hf_3O
0.92	Annealed	6.20	VW	Ta_2O_5
		5.03	W	HfO_2
		3.60	W	HfO_2; Ta_4O
		3.13	W	HfO_2; WO_3
		2.962	VS	Ta_2O
		2.794	VW	Hf_3O
0.92	Annealed	2.597	W	HfO_2
		2.503	M	Hf_3O; WO_3
		2.325	VW	HfO_2; Ta_6O
		2.285	VW	Ta_4O
		2.040	VW	WO_3
		1.802	S	Ta_2O_5; Ta_4O; HfO_2
		1.768	M	HfO_2; Ta_2O_5
		1.698	VW	WO_2
		1.656	W	HfO_2; Ta_2O
		1.639	VW	WO_3; HfO_2
		1.555	M	Hf_3O; WO_3; Ta_2O_5
		1.514	S	Hf_3O
		1.463	W	WO_2; Ta_2O_5; HfO_2
		1.371	VW	Ta_2O_5; WO_3
		1.312	VW	Ta_2O_5
		1.260	W	WO_3; HfO_2; Ta_2O
		1.233	W	Hf_3O; HfO_2
		1.172	M	Ta_6O; HfO_2
		1.154	W	HfO_2
		1.129	W	Ta_4O
		1.125	W	Ta_2O_5; HfO_2
		1.088	VW	Ta_6O; HfO_2
		1.050	VW	HfO_2; Ta_2O_5
		1.032	W	Ta_6O
		1.001	W	Hf_3O
2.97	Annealed	6.10	VW	Ta_2O_5
		5.09	VW	HfO_2
		3.60	M	HfO_2; Ta_4O
		3.13	M	HfO_2
		2.966	VS	Ta_2O
		2.820	M	HfO_2; WO_2
		2.597	M	HfO_2
		2.506	M	Hf_3O; WO_3
		2.325	W	HfO_2; Ta_6O
		2.285	W	Ta_4O
		2.040	W	WO_3
		1.804	S	HfO_2; Ta_4O; Ta_2O_5
		1.768	M	HfO_2; Ta_2O_5
		1.697	W	WO_2
		1.635	W	HfO_2; Ta_4O; Ta_2O_5
		1.551	M	Hf_3O; WO_3; Ta_2O_5
		1.507	VW	HfO_2
		1.464	M	Ta_2O_5; WO_2; HfO_2
		1.441	VW	Ta_2O_5; HfO_2
		1.410	VW	WO_2; HfO_2
		1.369	VW	WO_3; Ta_6O
		1.341	VW	Ta_2O_5; Ta_6O
		1.306	VW	Ta_2O; TaO_2
		1.258	M	Ta_2O; HfO_2
		1.200	VW	WO_2; HfO_2
		1.173	M	HfO_2; Ta_6O; Ta_2O
		1.151	W	Ta_2O_5; HfO_2
		1.125	S	Ta_4O; Ta_2O_5
		1.103	VW	HfO_2
		1.088	W	Ta_6O; HfO_2
		1.050	W	HfO_2; WO_3
		1.032	M	Ta_6O
		1.000	W	Hf_3O

[a] At 1320° C for 2 hr.

[b] M, medium; S, strong; W, weak; V, very.

TABLE V. - X-RAY DIFFRACTION PATTERNS FOR OXIDE EXTRACTED FROM NONANNEALED AND ANNEALED[a] OXYGEN-DOPED T-111 ALLOY SAMPLES AT 990° C

Oxygen concentration, at. %	T-111 condition	d-Spacing, Å	Intensity (b)	Oxide
0.43	Nonannealed	6.60	VW	Ta_2O
		5.05	W	HfO_2
		3.61	W	Ta_4O, HfO_2
		3.46	W	WO_2
		2.961	VW	Ta_2O
		2.832	W	HfO_2, WO_2
		2.717	W	Ta_2O
		2.589	M	HfO_2, Hf_3O
		2.482	M	HfO_2
		2.285	W	Ta_4O
		1.802	S	HfO_2, Ta_4O, Ta_2O_5, WO_3
		1.768	M	HfO_2, Ta_2O_5
		1.656	VS	HfO_2, Ta_2O_5, Ta_2O
		1.639	W	WO_3, HfO_2, Ta_2O_5
		1.549	W	WO_2
		1.523	M	Ta_2O
		1.515	S	Hf_3O
		1.469	M	HfO_2, Ta_2O_5, Ta_6O, WO_2
		1.269	W	Ta_2O, HfO_2
		1.256	M	HfO_2
		1.173	W	Ta_6O, HfO_2, Ta_2O_5
		1.158	W	Ta_2O
		1.127	M	Ta_4O
		1.049	W	HfO_2
		1.033	W	Ta_2O
		1.002	W	Hf_3O
0.97	Annealed	6.20	VW	Ta_2O_5
		5.06	W	HfO_2
		3.61	M	HfO_2, Ta_4O
0.97	Annealed	3.09	W	Ta_2O_5, WO_3
		2.961	M	Ta_2O
		2.802	W	Hf_3O, HfO_2
		2.597	M	HfO_2
		2.503	M	Hf_3O, WO_3
		2.325	W	HfO_2, Ta_6O
		2.286	↓	Ta_4O
		2.120		Ta_2O, Ta_2O_5
		2.057		Ta_2O
		2.036		WO_3
		1.923		Ta_6O, Ta_2O
		1.852		Ta_2O, WO_2
		1.799	VS	Hf_3O, HfO_2, Ta_2O_5, WO_3, Ta_4O
		1.679	S	HfO_2, Ta_6O, Ta_2O_5
		1.600	W	HfO_2, Ta_4O, WO_2
		1.555	M	Hf_3O, WO_3, Ta_2O_5
		1.514	S	Hf_3O
		1.463	M	HfO_2, Ta_2O_5, WO_2, Ta_4O
		1.371	W	Ta_2O_5, WO_3, Ta_6O
		1.345	M	Ta_6O
		1.264	M	Ta_2O, HfO_2
		1.233	W	Ta_2O_5, Hf_3O, Ta_2O
		1.172	M	Ta_2O_5, Ta_6O, HfO_2
		1.130	M	Ta_4O, HfO_2
		1.124	W	Ta_2O_5
		1.087	W	HfO_2, Ta_2O
		1.051	W	Ta_2O_5
		1.032	M	Ta_6O, Ta_4O
		1.001	M	Hf_3O

[a] At 1320° C for 2 hr.

[b] M, medium; S, strong; W, weak; V, very.

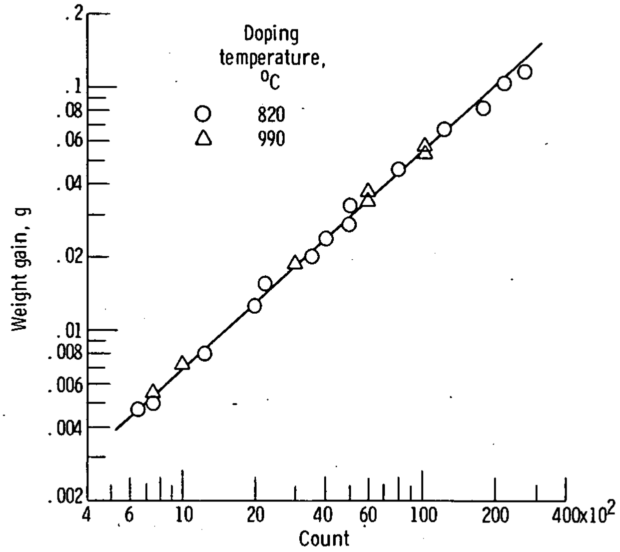

Figure 1. - Typical calibration curve for oxygen doping of T-111 tantalum alloy sheet specimens at a specific oxygen pressure by flux limited method.

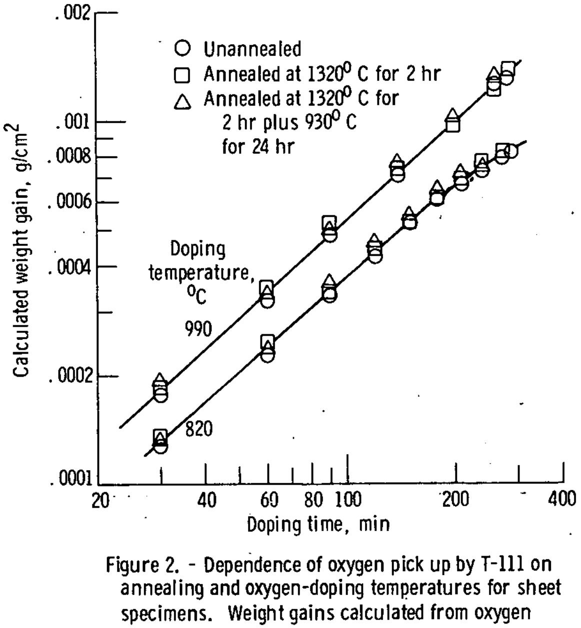

Figure 2. - Dependence of oxygen pick up by T-111 on annealing and oxygen-doping temperatures for sheet specimens. Weight gains calculated from oxygen counts using relationship shown in figure 1.

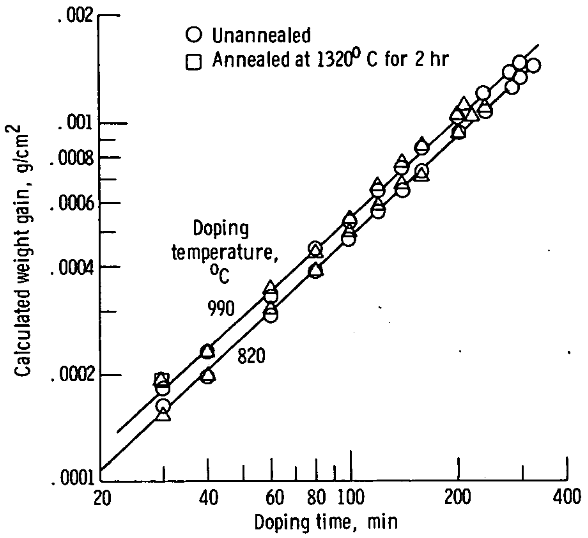

Figure 3. - Dependence of oxygen pick up by Ta-2Hf on annealing and oxygen-doping temperatures for sheet specimens. Weight gains calculated from oxygen counts using a curve similar to that of figure 1 but obtained for Ta-2Hf.

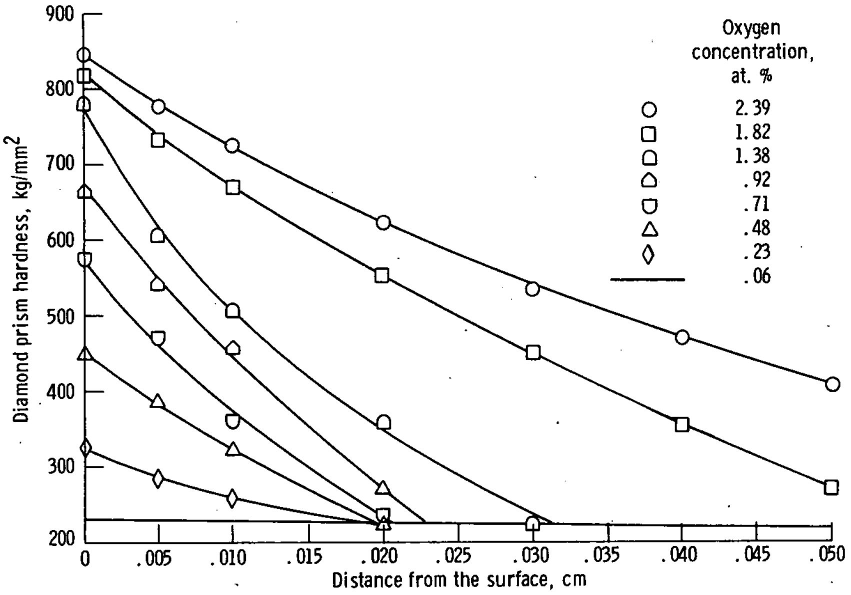

Figure 4. - Microhardness traverses for the T-111 tantalum alloy samples doped with oxygen at 820° C.

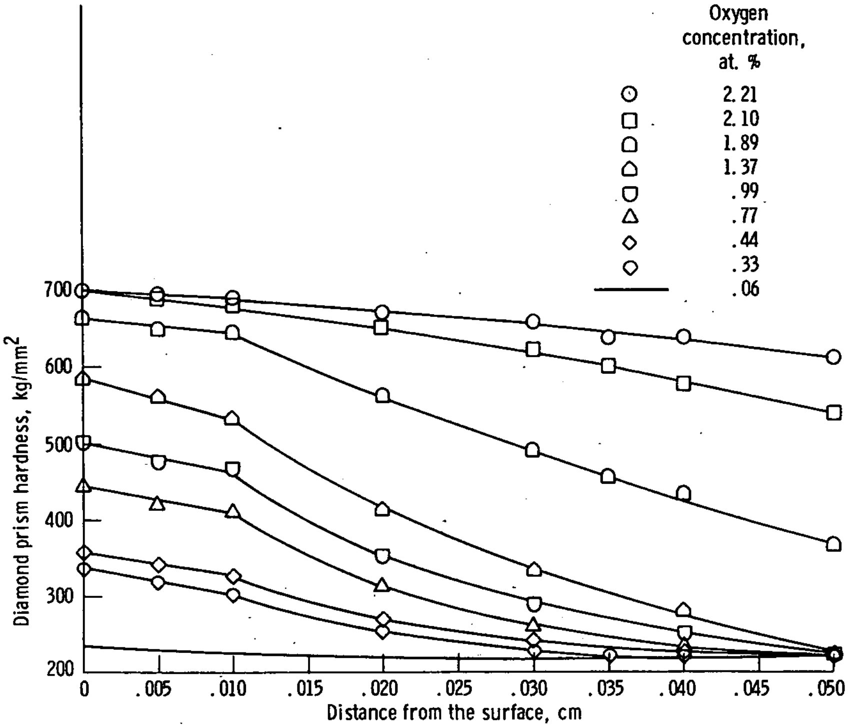

Figure 5. - Microhardness traverses for the T-111 tantalum alloy samples doped at 990° C.

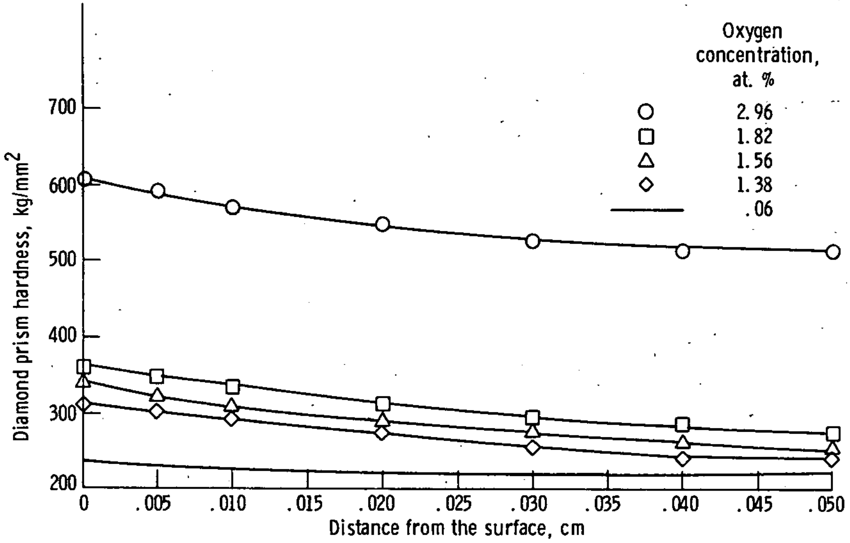

Figure 6. - Microhardness traverses for the T-111 tantalum alloy samples doped with oxygen at 820° C and annealed at 1320° C for 2 hours.

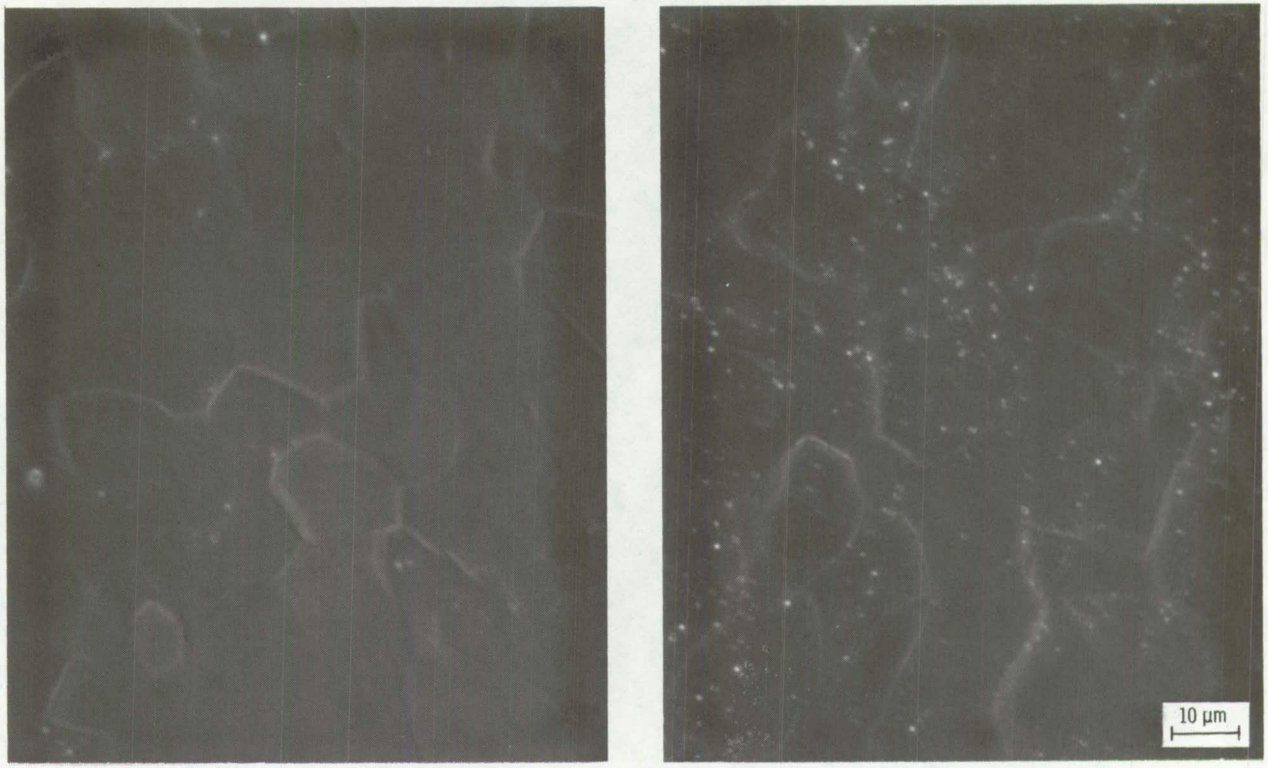

(a) Sample oxygen concentration, 0.65 atomic percent.

(b) Sample oxygen concentration, 1.20 atomic percent.

Figure 7. - Optical microscope polarized-light photomicrograph showing presence of second phase in T-111 alloy doped at 820° C.

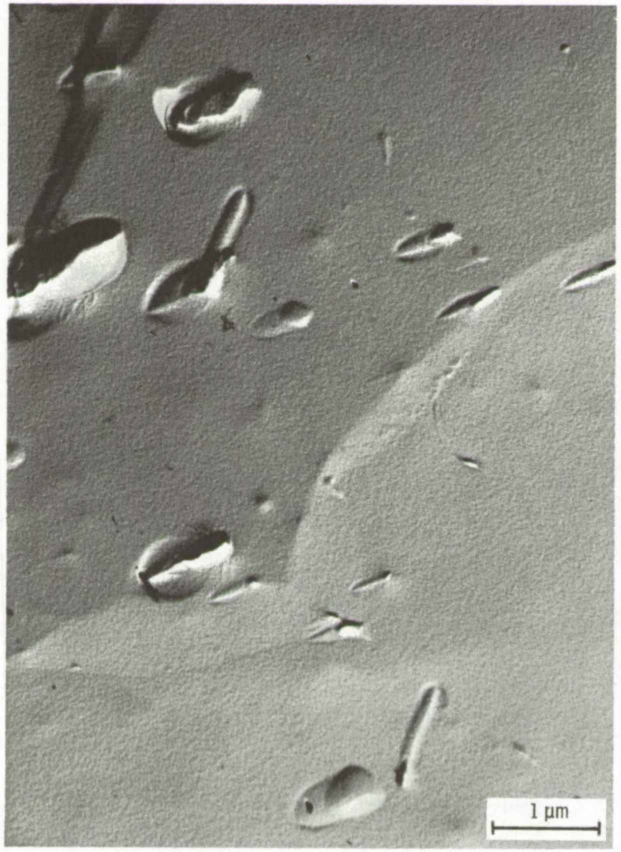

Figure 8. - Transmission electron photomicrograph of oxide particles in T-111 alloy doped at 820° C and containing 0.65 atomic percent oxygen

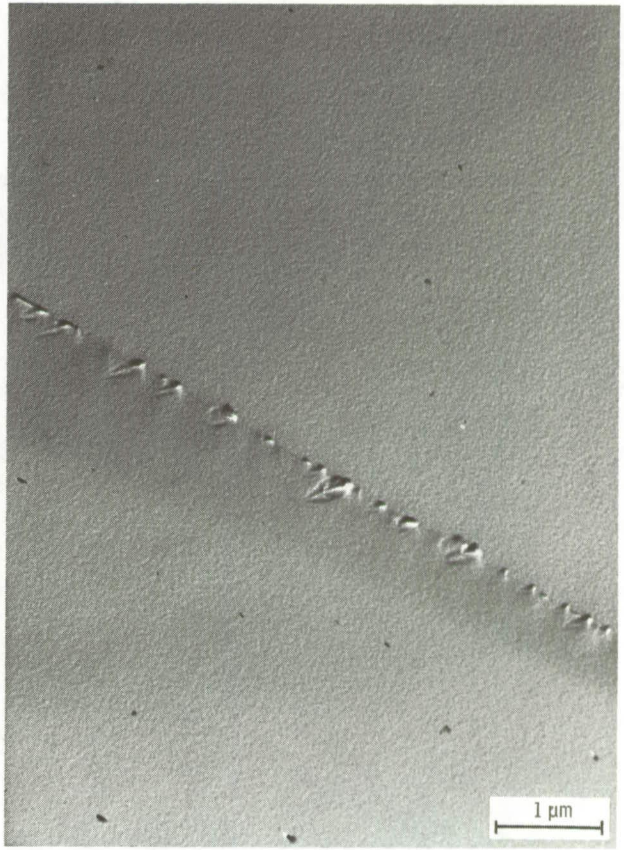

Figure 9. - Transmission electron photomicrograph of oxide particles at grain boundaries in T-111 alloy doped at 820° C and containing 0.65 atomic percent oxygen.

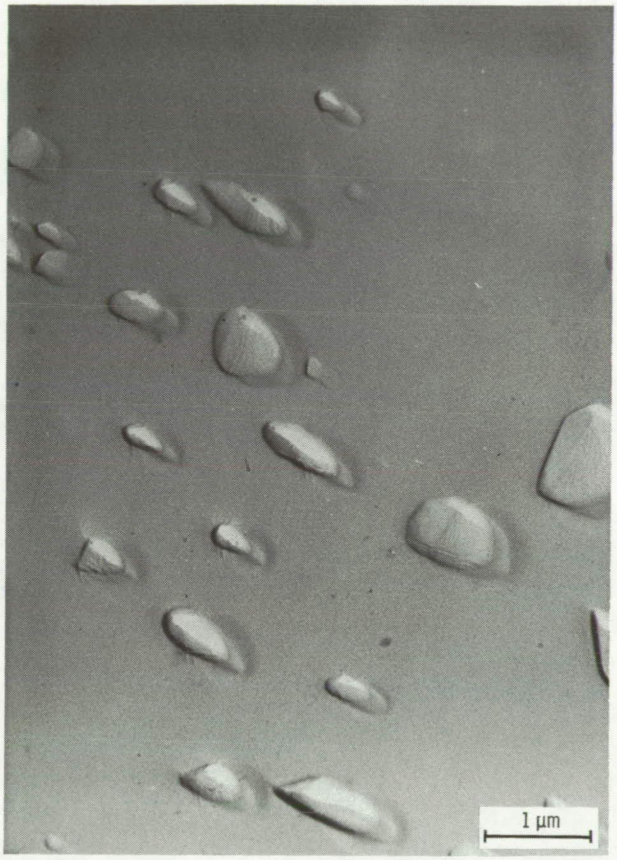

Figure 10. - Transmission electron photomicrograph of oxide particles in T-111 alloy doped at 820° C and containing 1.29 atomic percent oxygen.

> *"The aeronautical and space activities of the United States shall be conducted so as to contribute . . . to the expansion of human knowledge of phenomena in the atmosphere and space. The Administration shall provide for the widest practicable and appropriate dissemination of information concerning its activities and the results thereof."*
>
> —NATIONAL AERONAUTICS AND SPACE ACT OF 1958

NASA SCIENTIFIC AND TECHNICAL PUBLICATIONS

TECHNICAL REPORTS: Scientific and technical information considered important, complete, and a lasting contribution to existing knowledge.

TECHNICAL NOTES: Information less broad in scope but nevertheless of importance as a contribution to existing knowledge.

TECHNICAL MEMORANDUMS: Information receiving limited distribution because of preliminary data, security classification, or other reasons. Also includes conference proceedings with either limited or unlimited distribution.

CONTRACTOR REPORTS: Scientific and technical information generated under a NASA contract or grant and considered an important contribution to existing knowledge.

TECHNICAL TRANSLATIONS: Information published in a foreign language considered to merit NASA distribution in English.

SPECIAL PUBLICATIONS: Information derived from or of value to NASA activities. Publications include final reports of major projects, monographs, data compilations, handbooks, sourcebooks, and special bibliographies.

TECHNOLOGY UTILIZATION PUBLICATIONS: Information on technology used by NASA that may be of particular interest in commercial and other non-aerospace applications. Publications include Tech Briefs, Technology Utilization Reports and Technology Surveys.

Details on the availability of these publications may be obtained from:

SCIENTIFIC AND TECHNICAL INFORMATION OFFICE

NATIONAL AERONAUTICS AND SPACE ADMINISTRATION

Washington, D.C. 20546